SOCIETY FOR EXPERIMENTAL BIOLOGY

Journal of Experimental Botany, Vol. 72, No. 10 pp. 3677–3687, 2021
doi:10.1093/jxb/erab111 Advance Access Publication 15 March, 2021

RESEARCH PAPER

How kelp in drag lose their ruffles: environmental cues, growth kinematics, and mechanical constraints govern curvature

Mimi A.R. Koehl[1,*] and Wendy K. Silk[2]

[1] Department of Integrative Biology, University of California, Berkeley, CA 94720-3140, USA
[2] Department of Land, Air, and Water Resources, University of California, Davis, CA 95616-5270, USA

* Correspondence: cnidaria@berkeley.edu

Received 28 July 2020; Editorial decision 2 March 2021; Accepted 12 March 2021

Editor: Yoel Forterre, CNRS Aix-Marseille University, France

Abstract

We reveal how patterns of growth in response to environmental cues can produce curvature in biological structures by setting up mechanical stresses that cause elastic buckling. *Nereocystis luetkeana* are nearshore kelp with wide ruffled blades that minimize self-shading in slow flow, but narrow flat blades that reduce hydrodynamic drag in rapid flow. Previously we showed that blade ruffling is a plastic trait associated with a transverse gradient in longitudinal growth. Here we consider expansion and displacement of tissue elements due to growth in blades, and find that growth patterns are altered by tensile stress due to hydrodynamic drag, but not by shading or nutrients. When longitudinal stress in a blade is low in slow flow, blade edges grow faster than the midline in young tissue near the blade base. Tissue elements are displaced distally by expansion of younger proximal tissue. Strain energy caused by the transverse gradient in longitudinal growth is released by elastic buckling once the blade grows wide enough, producing ruffles distal to the region where the growth inhomogeneity started. If a blade experiences higher stress in rapid flow, the edges and midline grow at the same rate, so the blade becomes flat as these new tissue elements are displaced distally.

Keywords: Buckling of thin plates, environmental plasticity, growth kinematics, kelp, morphogenesis, stress adaptation.

Introduction

Curved and twisted forms are common in nature (Thompson, 1917). The theory of elastic thin plates and shells has illuminated a diversity of mechanisms that produce curved forms in different organisms and structures, including curving leaves (e.g. Moulia *et al.*, 1994; Sharon *et al.*, 2002; Nath *et al.*, 2003; Jakubska-Busse *et al.*, 2016; Gao *et al.*, 2019) and flowers (Liang and Mahadevan, 2011; Woollacott *et al.*, 2019), uncurving notochords of frog embryos (Koehl *et al.*, 2000), ruffled kelp (Fig.

Abbreviations: $L(x,t)$, the length of a material tissue element as a function of position and time, a Lagrangian specification; $t(X,x)$, time required for X to arrive at position x, a Lagrangian specification; $v(x)$, longitudinal growth velocity (displacement rate), shown as an Eulerian specification; x, distance from the origin at the frond base (longitudinal coordinate); X, name of a tissue particle found initially at X cm from the frond base; $x(X,t)$, the location of X followed through time, a Lagrangian specification; $\delta v/\delta x$, longitudinal growth strain rate (relative elemental growth rate) shown as an Eulerian specification; ε, extra length of a lateral tissue element relative to an element on the midline, a Lagrangian specification.

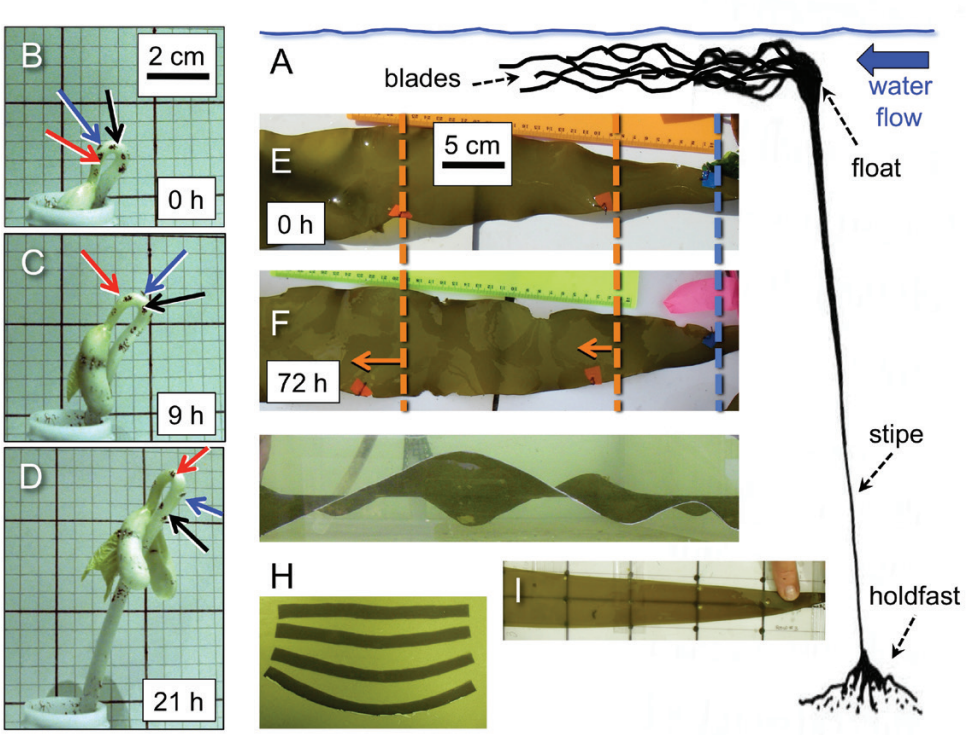

Fig. 1. Contrast between the 'spatial' curvature of a seedling hook and the 'material' curvature of ruffles on a kelp blade. (A) Diagram of a *N. leutkeana*, showing blades held up by a float in flowing water. (B–D) Marks (indicated by colored arrows) on the seedling hook of *Phaseolus vulgaris* flowed through the form as the plant grew; the hook was composed of a procession of changing tissue elements, each of which first curved and then straightened during its displacement from the plant apex. The hook remained a fixed distance from the apex. (E and F) In contrast, tags sewn onto kelp ruffles (orange tags; positions at time t=0 h shown by dashed lines) remained in the ruffles. The curved form was displaced from the blade base (blue tag, position at t=0 h shown by a dashed line), and eventually occupied the distal mature region of the blade. (G) Side view of a ruffled kelp blade from a slow-flow habitat. (H) When narrow (1 cm wide) strips were cut from a ruffled blade and flattened, the outer strips had non-zero curvature equal to the geodesic curvature of the blade edge (Sharon *et al.*, 2007). (I) Flat blade from a current-swept site. (2 cm scale bar for B–D; 5 cm scale bar for E–I).

1A; Koehl *et al.*, 2008), twisting bacteria (Wolgemuth *et al.*, 2005) and plant tendrils (Bowling and Vaughn, 2009; Gerbode *et al.*, 2012), twining vines (Silk and Hubbard, 1991; Isnard and Silk, 2009; Isnard *et al.*, 2009), helical splitting of seed pods (Armon *et al.*, 2011), insect trapping by snap-buckling leaves (Forterre *et al.*, 2005), self-burying by bending awns on seeds (Elbaum *et al.*, 2007; Aharoni *et al.*, 2012), bending tropisms of plants (Bastien *et al.*, 2018; Meroz *et al.*, 2019), and even coiling nanoparticulate rods (reviewed in Chen *et al.*, 2016). A general principle unifying these studies is that in thin forms, such as sheets or rods, the mechanical energies (i.e. elastic strain energies) stored in the structure during bending and twisting are lower than stretching energies. Therefore, the structures elastically take on curved or twisted shapes of lower strain energy when non-homogeneous swelling or shrinking of the structure occurs during growth, or via water uptake or loss. In particular, doubly curved structures have several shapes of minimal energy, with obligate coupling between transverse and longitudinal curvatures (Moulia, 2000; Zhao *et al.*, 2019). In all of these shape changes, mechanical constraints are seen to determine the morphogenesis, while the involvement of genes must be relegated to controlling tissue physical properties such as geometry, growth rate, and the arrangement of inextensible fibers in the structure.

Collectively the studies of how elastic behavior can produce curved and twisted biological shapes represent a major advance in our understanding of biological form; however, few incorporate the spatio-temporal patterns of growth that can set up the stresses driving these changes in shape. Nineteenth and twentieth century studies of morphogenesis of plant form revealed a general principle that is rarely incorporated into the emerging theory of elastic generation of curvature in organisms. Classical botanists recognized the developmental gradient inherent in plant structure (reviewed by Lyndon, 1990). Cell division and expansion are most often localized in apical regions in roots and shoots, and in leaf bases in grasses. Cells are displaced by the growth of their younger neighbors. Kinematic analysis of growth involves both Eulerian, site-specific considerations (determining changes with time at fixed spatial positions, such as distance from a root or shoot apex), and Lagrangian, tissue-specific analyses (following marked tissue elements to determine how, for example, their velocities, chemistry, and growth

change as a function of time and position) (Green, 1976; Silk and Erickson, 1979; Gandar, 1983; Silk, 1984). Such growth analyses reveal whether curved structures are 'material' or 'spatial' entities. A curved material entity is formed and maintained in a segment of tissue, but the position of that curved tissue segment within the structure can be changed by the growth of neighboring tissue. Such a developmental pattern produces the longitudinal curvature of the maize leaf distal to the primary growth zone (Hay *et al.*, 2000). In contrast, the position of a curved spatial entity is fixed within a structure as a sequence of tissue elements grow through the curved shape. The hooks of dicotyledonous seedlings (Silk and Erickson, 1978) and growing compound leaves (Rivière *et al.*, 2020) are examples of such spatial entities (Fig. 1B–D). These hooks have a quasi-steady spatial curvature field with a curvature maximum maintained a fixed distance from the apex of the structure. Tissue elements produced near the apex move through the curved shape as they grow, experiencing first a large increase, and then a large decrease in curvature during their growth displacement.

Many types of seaweeds can change their shape in response to environmental cues (reviewed in Koehl, 1986; Koehl *et al.*, 2008; Burnett and Koehl, 2019), so they provide useful biological systems to combine elasticity theory with spatio-temporal analysis of developmental gradients to study how the kinematics of growth can produce or eliminate curvature. Some species of seaweeds, including the giant bull kelp *Nereocystis luetkeana* (Mertens) Postels and Ruprecht, have flat blades in habitats exposed to rapid water currents, but ruffled and/or twisted blades at calmer sites (Koehl and Alberte, 1988; Koehl *et al.*, 2008). Koehl and colleagues have identified the functional significance of the different morphologies (Koehl and Alberte, 1988; Koehl *et al.*, 2008). In habitats with slow currents (peak velocities ~0.5 m s^{-1}), the kelp forms wide, ruffled blades (Fig. 1E–H) that spread out and flutter in moving water, thereby maximizing the area exposed to light, but also resulting in large hydrodynamic drag. (When hanging vertically in still water, the ruffled blades exhibit slightly twisted shapes.) In contrast, at sites exposed to fast water currents (peak velocities ~1.5 m s^{-1}), *N. luetkeana* produces narrow, flat blades (Fig. 1I) that are pushed together by ambient water flow into streamlined bundles that minimize drag and associated breakage, but decrease light interception due to self-shading within the bundle. Kelp, which have no roots, depend on uptake of dissolved substances from the surrounding water. Such uptake by kelp blades is reduced in slow ambient water flow (e.g. Koehl and Alberte, 1988; Hurd, 2000), but fluttering in slow currents can enhance uptake by both flat and ruffled blades (Koehl and Alberte, 1988). Transplant experiments in the field revealed that the shape of the blade in *N. luetkeana* is a plastic trait, and lab experiments showed that the ruffles are produced by elastic buckling (Koehl *et al.*, 2008).

We took advantage of the ability of *N. leutkeana* to change blade shape in response to flow environment to study how the kinematics of blade growth can produce flat tissue or ruffles caused by elastic buckling. We used a Lagrangian analysis of growth in which we followed tissue elements to determine how their expansions and their displacements in the blade structure (due to growth of proximal tissue) changed as a function of time and position in blades that were producing ruffles versus in blades that were producing flat tissue in response to environmental cues. The specific questions that we addressed were as follows. (i) Are the ruffles of *N. leutkeana* blades 'material' or 'spatial' entities? A tissue segment that retains a ruffled morphology throughout its displacement in a growing blade is a material entity, whereas a ruffle at a particular location on a blade that is occupied by tissue that is buckled only during its transit through that region is a spatial entity. (ii) What are the growth kinematics that produce ruffled versus flat blades? (iii) How do growth kinematics change when a blade alters its shape in response to flow environment? (iv) Which environmental cues that correlate with flow environment (tensile stress due to drag, light reduction due to self-shading, or nutrient uptake from the surrounding water) affect growth kinematics and blade ruffling?

Materials and methods

Research species

We studied the diploid sporophyte of the annual kelp, *Nereocystis luetkeana* (Mertens) Postels and Ruprecht. Kelp (Order Laminariales) are brown algae (Class Phaeophyceae). The sporophyte of *N. leutkeana* grows in dense stands to depths of 3–17 m in Pacific coastal waters from Alaska to central California (Abbott and Hollenberg, 1976). A holdfast anchors the alga to the ocean floor; a long cylindrical stipe terminates in a gas-filled float that holds many (30–60) photosynthetic blades (as long as 4 m) near the water surface (Fig. 1A). Meristematic tissue generates new cells at the base of the blades.

Field sites

The field experiments described below were conducted in beds of *N. luetkeana* near Friday Harbor, San Juan Island, WA, USA (48.5343°N, 123.0171°W), at a 'current-swept site' that was exposed to rapid tidal currents with peak speeds of 1.5 m s^{-1} (Turn Rock), and at a 'protected site' (Shady Cove) at which peak tidal currents were only 0.5 m s^{-1} (flow data in Koehl and Alberte, 1988; Johnson and Koehl, 1994; Koehl *et al.*, 2008). Kelp collected from these two sites were used in the dock and tank experiments described below. In all cases, collected kelp were those within reach of a boat anchored in the kelp bed.

Determination of whether ruffles are spatial or material entities

The concept of the ruffle being a spatial or material entity is nuanced. The ruffle itself is floppy and, because it is formed by elastic buckling, can exist in several configurations with short or longer wavelengths (Koehl *et al.*, 2008). Therefore, we used a repeatable operational definition of a ruffle for this study: a ruffle was a region of the blade edge that buckled up off a flat surface on which a blade was laid (Fig. 2). The existence of a tissue segment that retains such a ruffled morphology throughout its displacement (a material entity) is fundamentally different from a ruffled

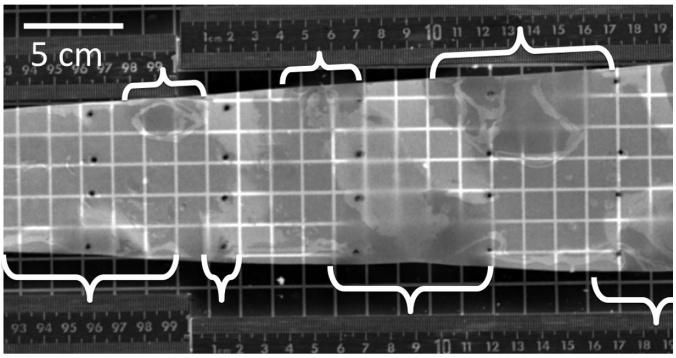

Fig. 2. Operational definition of a ruffle. When a blade was laid out onto a flat surface, the regions of the blade that buckled up above the surface were defined as ruffles. Brackets indicate the ruffles in this photograph of a blade laid on a flat grid, which can be seen through the translucent blade tissue. Some of the holes punched in the blade are shown.

region occupied by tissue that is buckled only during its transit through the region (a spatial entity).

Five *N. leutkeana* were collected from the protected site. On the first day of this study, we picked one undamaged blade on each kelp and laid it flat on the dock. We stitched a 1 cm tag of flagging tape to the peak of each ruffle on the blade and photographed it (Fig. 1E). Then the kelp were hung from the dock at Friday Harbor Laboratories, where they were exposed to slow water motion (flow data in Hunter, 1988) similar to that at the protected site (flow data in Koehl and Alberte, 1988). Photographs of the marked blades were taken every 24 h for 5 d (e.g. Fig. 1E, F) and the positions of the tagged tissue and the ruffles were noted.

Measurements and numerical methods to quantify growth kinematics that produce ruffled versus flat blades

Growth velocity and growth strain rate fields

We measured the position changes with time of a grid of holes punched in growing blades (Fig. 2) and calculated the velocities at which they moved away from the blade origin at the pneumatocyst (float), analogous to an Eulerian analysis in fluid dynamics (Fig. 3A). Longitudinal growth velocities (v, mm d^{-1}) as a function of x (longitudinal distance, cm, from the blade origin) were calculated from measurements of the longitudinal displacement of holes punched in growing blades of *N. luetkeana* living at the protected site and at the current-swept site. At each site, a boat was anchored in the kelp bed. The pneumatocyst and attached blades of kelp within reach of the boat were pulled onto the deck. One blade of each plant was placed on a marked x,y grid that served as a template for a grid of holes punched into the blade by a hollow brass rod 2 mm in diameter. Holes were punched at 5 cm intervals from the blade origin along the blade midline. A ruler was laid across the blade laterally at each interval to hold that position of the blade flat onto the grid while allowing the blade to buckle proximally and distally from the ruler, and holes were punched 2 cm lateral to the midline, and along one blade edge. Because only the proximal portion of an *N. leutkeana* blade grows (Koehl *et al.*, 2008), this grid of holes was punched into the proximal 65 cm of each blade. Curvilinear distances between holes were measured to the nearest millimeter with a flexible tape measure. These kelp were identified with numbered plastic flagging tape tied to the pneumatocyst and were left to grow *in situ* for 6 d. After the growth period, the marked blades were collected and taken to a laboratory where the final curvilinear distances between holes were measured to the nearest millimeter with a flexible tape measure. For each of n blades in the treatment, growth velocity was calculated as the displacement of the holes from the origin, divided by the number of days of growth. The velocity field $v(x)$ was interpolated to the millimeter scale with the MATLAB interp1 routine and was recorded as a function of initial position on the blade. Mean values and SDs were calculated for each treatment for graphical display. For each blade, the growth velocity field was differentiated with respect to position using the MATLAB diff routine to compute the local relative growth rates of tissue elements as a function of position (Erickson and Sax, 1956) analogous to the strain rate field of fluid dynamics (Fig. 3B); mean values and SDs for each treatment were calculated for graphing. Such growth rate fields are used by physiologists to compare with spatial distributions of putative growth-regulating agents (hormones, chemical composition, or mechanical properties) to discover the mechanisms for growth regulation (e.g. Phyo *et al.*, 2017; Rabille *et al.*, 2019).

Growth trajectories and tissue segment lengths

Assuming a quasi-steady growth velocity field and integrating the velocity of a tissue particle over time, we could by computation 'follow' tissue elements as they moved and plot their distances from the blade origin as a function of time, similar to a Lagrangian analysis in fluid dynamics (Fig. 3C). Such 'growth trajectories' are a material description of growth (analogous to the particle pathlines of fluid dynamics) and provide a space–time map for developmental variables (Green, 1976; Silk and Erickson, 1979; Gandar, 1983; Silk, 1984; Bastien *et al.*, 2018). Neighboring tissue particles separate from each other as the tissue grows. Thus growth trajectories of neighboring tissue particles can be used to calculate the expanding length of a tissue element as it is displaced in space and time (Fig. 3C, D). For example, a tissue segment initially 1 cm long and located with its proximal end 5 cm from the blade base elongates to be 3.7 cm during its displacement for 21 d through the 60 cm growth zone (Fig. 3D).

We use the continuum mechanical notation $x(X,t)$ to represent the growth trajectory of particle X. The particle is designated by its initial position X (cm from base of the kelp blade at t=0). Thus $x(5,t)$ is the function giving the position over time of the tissue particle initially found at 5 cm. This growth trajectory is displayed as the lowest line in Fig. 3C. This is a material (cell particle-specific rather than site-specific) description of growth and provides a space–time map for developmental variables. The inverse function $t(5,x)$ gives the time during which the particle that was initially at 5 cm is displaced to distal locations on the blade. The interpolated velocity field $v(x)$ for each individual blade (see preceding section) was used to calculate displacement times of particles located initially at X by numerical integration of the millimeter-spaced velocities following the particle through time and space,

$$t(X,x) = \sum_{x}^{x(t)} \left(\frac{1}{V(x)} \right) \tag{1}$$

Growth trajectories $x(X,t)$ were then calculated by interpolating $t(X,x)$ to equally spaced times with the MATLAB interpol1 routine, as shown in Fig. 3C. Assuming a quasi-steady growth velocity field, we computed the length of a tissue element during its displacement. As illustrated in Fig. 3D, for the segment initially 1 cm long and lying between 5 cm and 6 cm from the base of the blade, the length at time t, $L(t)$, is given by:

$$L(t) = [x(6,\ t) - x(5,t)] \tag{2}$$

(Fig. 3C, D). The temporal patterns $L(t)$ were then mapped back to the spatial domain using the growth trajectory $x(5,t)$ to obtain $L(x)$, and segment length was displayed as a function of position to allow comparison with other morphological, anatomical, and physiological properties of interest. Growth trajectories $x(X,t)$ and segment lengths $L(x)$ were computed for each blade; means were calculated for each treatment for graphical display.

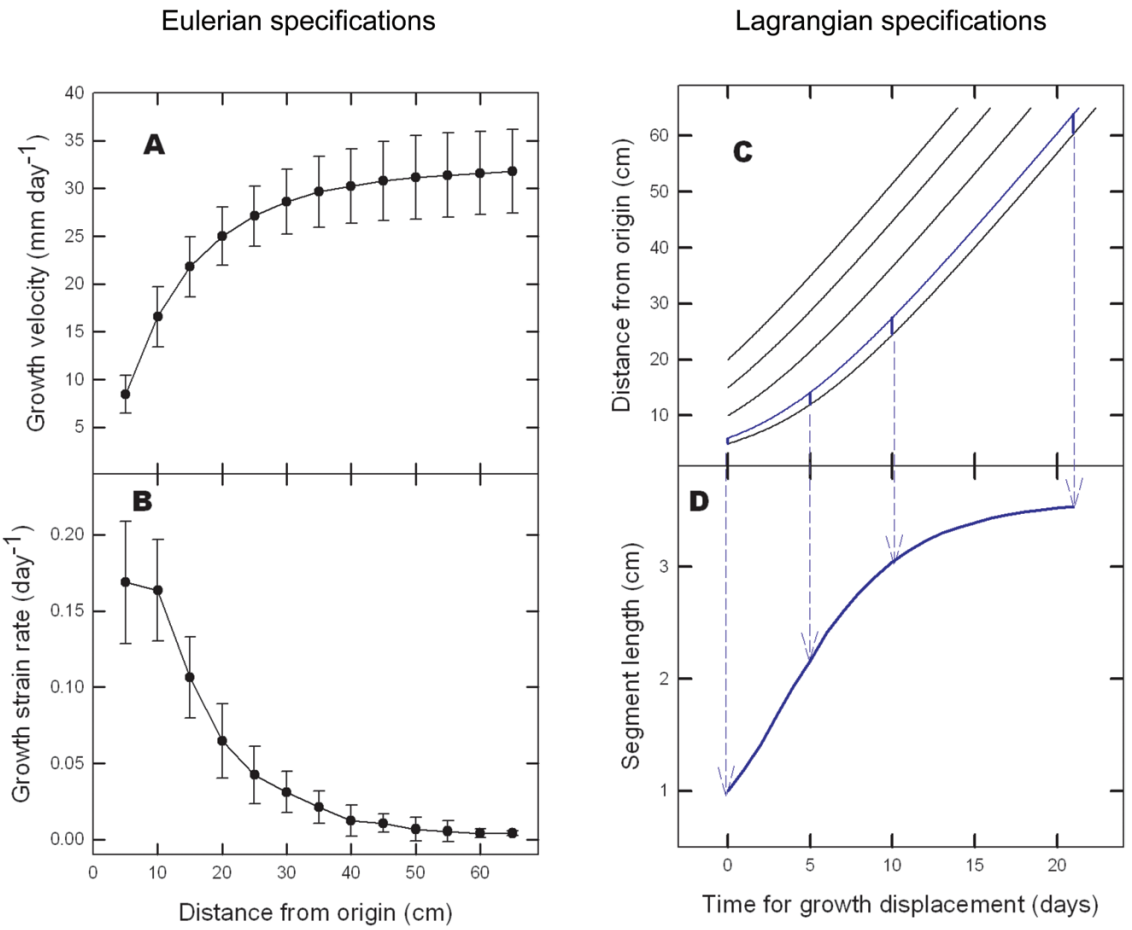

Fig. 3. Example of growth kinematics to find the length of tissue elements over time. Data are from marking experiments on kelp blades growing at a field site with slow ambient water currents (± 1 SD, *n*=one blade on each of five kelp). (A) The longitudinal growth velocity field $v(x)$ was numerically differentiated to find (B) the field of growth strain (i.e. relative elemental growth) rates, $\delta v/\delta x$. This is the spatial (Eulerian) pattern of the instantaneous growth rate. (C) Assuming a quasi-steady growth velocity field and integrating the velocity of a tissue particle over time, we could by computation 'follow' tissue elements as they moved and plot their distances from the blade origin as a function of time, similar to a Lagrangian analysis in fluid dynamics. Each line represents the growth trajectory of an element of tissue that started at a different distance from the origin at t=0. Tissue particles accelerated through the growth zone as shown in the growth trajectories, $x(X,t)$, plots of position x of particle X versus time t. (D) Example of how a tissue element, initially extending from 5 cm to 6 cm from the base of the blade, increased in length for 20 d during its displacement through the 60 cm growth zone. (C) and (D) show Lagrangian specifications, following a material tissue element during its growth and displacement.

Ruffling

To analyze ruffle formation, we consider the pattern of longitudinal growth across the width of the blade. Ruffles can form by elastic buckling in thin ribbons if the tissue has grown more at the edges than along the midline of the blade (Sharon *et al.*, 2002; Nath *et al.*, 2003; Koehl *et al.*, 2008; Liang and Mahadevan, 2009; Gao *et al.*, 2019; Woollacott *et al.*, 2019). In our discussion of ruffle formation we will use 'transverse growth gradient' to refer to longitudinal growth that increases from the midline to the edge of a blade. This is quantified by comparing the longitudinal growth of the tissue element lying 2 cm from the midline to the longitudinal growth of an element at the same longitudinal position along the midline (Fig. 4). We calculated a relative length difference, 'extra lateral growth', $\varepsilon(x)$.

$$\varepsilon\,(x) = \frac{L(x)_{\text{lateral}} - L(x)_{\text{midline}}}{L(x)_{\text{midline}}} = \frac{L(x)_{\text{lateral}}}{L(x)_{\text{midline}}} - 1 \qquad (3)$$

Elasticity theory for flat plates predicts that for a given ε the edges of a ribbon-like blade are more likely to buckle into ruffles if the ratio of blade width (W) to blade thickness (t) is high (e.g. Liang and Mahadevan, 2009). Vernier calipers were used to measure the thickness of blades of *N. leutkeana* (to the nearest 0.1 mm) at intervals of 5 cm along the length of each blade used for growth measurements. After the *in situ* growth experiments described above were completed, blades into which holes had been punched were collected, laid flat on a surface, and photographed. For blades in which ruffles were found, the distance from the blade base at which the first ruffle was located was measured to the nearest millimeter, as was the width of the blade at the site where the first ruffle was located.

Quantification of changes in growth kinematics when blades alter shape in response to flow environment

We analyzed blade growth as described above for *N. leutkeana* transplanted to different flow habitats. Five kelp with wide, ruffled blades collected from the protected site were transplanted to the current-swept site, and five kelp with narrow, flat blades collected at the current-swept site

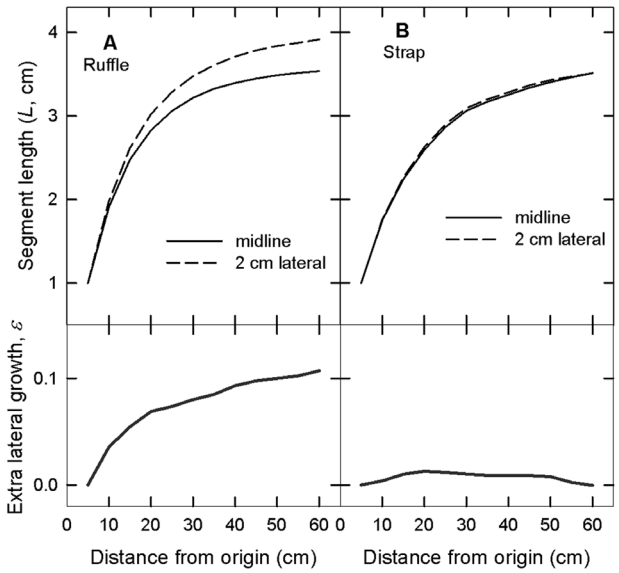

Fig. 4. Kinematics of ruffle versus strap formation. (A) For ruffle formation, the segment elongation is greater near the edge than along the midline of the blade. A length difference (ε) between tissue segments 2 cm lateral to the midline and tissue segments along the midline arises during growth displacement of the segment in blades growing at a slow-current site (computations based on growth velocity data for one blade on each of six kelp, as described in the Materials and methods). (B) The growth strains along the midline and near the margin were similar (there was no transverse growth gradient) in flat blades growing at a fast-current site (computations based on the growth velocity data for one blade on each of nine kelp, as described in the Materials and methods). Tests of significance were based on growth velocity data as described in the Results.

were transplanted into the protected site. Transplanted kelp were tied to cinder blocks on the substratum that held them in place at water depths where their pneumatocysts could float at the air–water interface. Grids of holes were punched into one blade per kelp, as described above, and the distances between holes were measured before the kelp were transplanted, and again after 6 d of growth in their new flow environments. Marked blades of kelp growing *in situ* at each site during the same 6 d period served as controls.

Determination of environmental factors that affect growth kinematics of blades

Blades on kelp at fast-current sites are subjected to higher mechanical loads due to hydrodynamic drag than are blades in slow-flow habitats, and to lower light intensity when they clump together in flow (Koehl and Alberte, 1988). Furthermore, uptake of dissolved substances by kelp blades is enhanced as ambient water flow velocities increase (e.g. Koehl and Alberte, 1988; Hurd, 2000). Therefore, mechanical stress due to drag, photon flux density (PFD) onto blades, and nutrient uptake are environmental factors that vary with ambient water flow and thus are candidates for the stimulus inducing changes in blade morphogenesis.

Effects of tensile stress on growth kinematics

Drag, the hydrodynamic force acting in the same direction as the water flow relative to a kelp blade, subjects it to tensile stress (force per cross-sectional area of tissue bearing the force). A study in which weights were hung on *N. leutkeana* blades in still water to determine the effect of tensile stress alone on blade shape showed that the blades from both current-swept and protected sites grew into flatter, narrower shapes when pulled (Koehl *et al.*, 2008). In the present study, we measured the effect of tensile stress in blade tissue on growth kinematics and blade shape by hanging weights on blades of kelp suspended in outdoor cylindrical plexiglass tanks (2 m tall and 1 m in diameter) with continuous flux of new seawater but no directional currents (fig. 10A in Koehl *et al.*, 2008). The drag per blade area on wide, ruffled blades of *N. leutkeana* from protected sites and on narrow, flat blades from current-swept sites has been measured at a range of flow velocities (Koehl and Alberte, 1988). These data were used to determine the tensile stress due to drag that blades of each shape would experience in water flow at our protected (0.5 m s^{-1}) and current-swept (1.5 m s^{-1}) sites, and to calculate the weight to hang on an individual blade that would produce the stress it would experience at the current-swept or the protected site. The end of a blade was protected by a plastic screen and was folded over and stitched together to make a loop, from which a weight was hung from twine threaded through that loop to evenly distribute the load across the width of the blade. This steady loading regime does not produce a stress (or strain) pattern identical to that induced by a fluctuating current *in situ*. Ruffled edges of a blade are not stretched as much as the unruffled blade midline when a blade is pulled by a weight suspended as described above. Also, a blade in ambient water flow flutters, whereas a weighted blade in our tank experiments does not, and the effect of fluttering on the magnitude of this difference in stretching between blade edges and midline is unknown. Nonetheless, the weighted blades, especially in unruffled regions including the flat meristem, did experience tensile stresses of similar magnitude to those produced by ambient currents at either the current-swept or the protected site.

For these tank experiments, a grid of holes (described above) was punched on three blades per kelp from the current-swept site (n=5 kelp) and from the protected site (n=5 kelp). For each kelp, a weight was hung on one blade that mimicked the stress due to drag it would experience at the protected site, another was hung with a weight that mimicked the stress due to drag it would experience at the current-swept site, and the third blade bore no weight. In addition, a common garden experiment was conducted in which kelp were collected from both sites (n=11 per site) and were grown in the experimental tanks without weights or current. A grid was punched onto one blade per kelp for these experiments. The growth kinematics for the tank experiments were analyzed as described above.

Effects of light on growth kinematics

To test whether the self-shading that occurs when kelp blades are pushed together by rapid ambient water flow could be an environmental cue that leads to loss of ruffling, we mimicked in our growth tanks the light reduction experienced by blades of *N. leutkeana* clumped together by rapid tidal currents. Field measurements showed that the photosynthetically active radiation (PAR) was ~30% of ambient for blades on *N. leutkeana* in currents of 1–2 ms^{-1} (Koehl and Alberte, 1988). Although little light reduction was measured in the field in clumps of ruffled blades fluttering in slower currents at the protected site (PAR was ~84% of ambient), field measurements of light among *N. leutkeana* blades hanging down during slack tide (similar to their configuration in our tank experiments) showed that PAR was ~30% of ambient (Koehl and Alberte, 1988). Therefore, to test the effects of shading on patterns of growth, five kelp from each site were hung in the middle of the tanks (described above) where they were shaded by surrounding kelp to mimic self-shading measured in the field in rapid flow (Koehl and Alberte, 1988). The clear plexiglas tanks were exposed to ambient sunlight. PFDs among the blades at mid-height in the tanks were measured every 2 h from sunrise (~05.00 h) until sunset (~21.00 h) during experiments in late June using a Biospherical Instruments QSI-140 Integrating Quantum Scalar Irradiance meter. Saturation PFD for photosynthesis for *N. luetkeana* blades is 110 μE m^{-2}

s^{-1}. (Koehl and Alberte, 1988). Shaded blades on kelp in tank centers were below saturation PFD for 36% of the time, whereas unshaded blades on kelp around tank peripheries were below saturation PFD for only 19% of the time. Grids were punched on one blade per kelp, and growth kinematics were analyzed as described above.

Effects of nutrients on growth kinematics

When *N. leutkeana* are not nitrogen limited, they store nitrate in their tissues, with the highest concentrations in blade tissue distal to the growth zone (Wheeler *et al.*, 1984). If slow water flow limits the uptake of nutrients, then the concentration of stored nutrients in blades from the protected Shady Cove site should be lower than in blades from the current-swept Turn Rock site. Therefore, the concentrations of stored nutrients (nitrate and phosphate) in the blade tissues distal to the growth zone of *N. leutkeana* from the current-swept and protected sites were measured to determine whether nutrient uptake differences between sites might affect blade growth kinematics. Analyses were conducted by the MSI Analytical Laboratory, University of California, Santa Barbara, for blade tissue samples collected in July and prepared and tested as described by Wheeler *et al.*, 1984.

Results

Are the ruffles of N. leutkeana *blades 'material' or 'spatial' entities?*

By following tagged ruffles on growing blades of *N. leutkeana* with time, we found that the curved ruffles of the blades form at distances of ~35–57 cm from the base of the blade and then are displaced distally as tissue proximal to them grows (n=5 blades, each from a different kelp, two ruffles tagged per blade, Fig. 1E, F). In every case, tags sewn on young ruffles remained in the ruffle during tissue displacement away from the blade meristem (Fig. 1E, F), even though the distance between young neighboring ruffles increased as a blade elongated and the ruffles became larger as they were displaced distally and blades grew wider. As discussed in the Introduction, the local ruffliness of the blade edge is therefore a property of the moving tissue element (i.e. is a material entity). Eventually, as they are displaced by the younger proximal tissue, the ruffles populate the mature, distal region of the blade.

What are the growth kinematics that produce ruffled versus flat blades?

The growth kinematics of ruffled blades from kelp at the protected site and of flat blades at the current-swept site were quantified. Growth velocities and strain rates were calculated for positions along a blade at fixed distances from the blade origin (Fig. 3A, B), and growth trajectories of tissue elements (Lagrangian specifications of distance from the blade origin over time) and the lengths of individual blade segments over time were calculated (Fig. 3C, D), as described in the Materials and methods. We used such data to compare the pattern of longitudinal growth across the width of a blade for kelp growing in the two different flow regimes. We found that only blades growing in slow currents that produced ruffles showed a transverse growth gradient, with blade edges elongating more rapidly than the blade midline (Fig. 4). In slow current, tissue 2 cm from the midline grew 5–12% more than tissue along the midline, whereas flat blades growing in rapid currents had growth along the midline indistinguishable from growth near the blade edge. For kelp in slow flow, the transverse growth gradient ε was evident by 10 cm from the base of a blade (corresponding to ~5 d of growth displacement; Fig. 3D), and increased in magnitude over the remaining 50 cm (21 d period) of displacement through the growth zone. Paired t-tests confirmed that in the proximal growth zone of blades, growth velocities (Fig. 3A) of lateral tissue were significantly faster than that of midline tissue for ruffled kelp blades growing in a slow-flow habitat (P=0.01, n=one blade on each of six kelp, df=5), whereas there was no difference between growth velocities of lateral and midline tissue for flat kelp blades growing at a rapid-current site (P=0.25, n=one blade on each of nine kelp, df=8). Note that the ruffles of the mature blade are not formed where they are eventually seen. Unlike the ruffling of an inanimate ribbon exposed to a transverse strain gradient along its entire length (e.g. Liang and Mahadevan, 2009), kelp ruffles are produced in one location, the proximal growth zone, and then displaced by younger tissue to form the mature blade.

The most recently formed ruffle (i.e. closest to the blade base) was observed in mid- to distal regions of the growth zone, as early as 35 cm and as late as 57 cm (Fig. 5). As described in the Materials and methods, theoretical considerations identify width and thickness as parameters that, together with the transverse gradient in longitudinal growth, determine the probability of ruffling. The thickness (t) of blades decreases with distance from the blade base, while blade width (W) increases (Fig. 5). In Fig. 5, the dimensionless parameter W/t is plotted as a function of distance from the blade base for ruffled blades growing at the protected site. The mean value of W/t at 48 cm (the mean position for first ruffle emergence) was 153.

How do growth kinematics change when a blade alters its shape in response to flow environment?

We analyzed the growth kinematics of ruffled blades on kelp transplanted from the protected site to the current-swept site, and of flat blades on kelp transplanted from the current-swept site to the protected site (Fig. 6A). Blades on kelp transplanted from a fast-current site to a slow-flow habitat developed a significantly higher growth velocity in lateral tissue than in midline tissue (paired t-test: P=0.01, n=one blade on each of five kelp, df=4), whereas blades on kelp transplanted from a calm habitat to a current-swept site showed no difference between lateral and midline growth velocities (P=0.06, n=one blade on each of five kelp, df=4). Computed values of ε show how lateral tissue expands more than midline tissue in the calm habitat in both native and transplanted kelp (Fig. 6A). These experiments and analyses confirm that the characteristic growth patterns

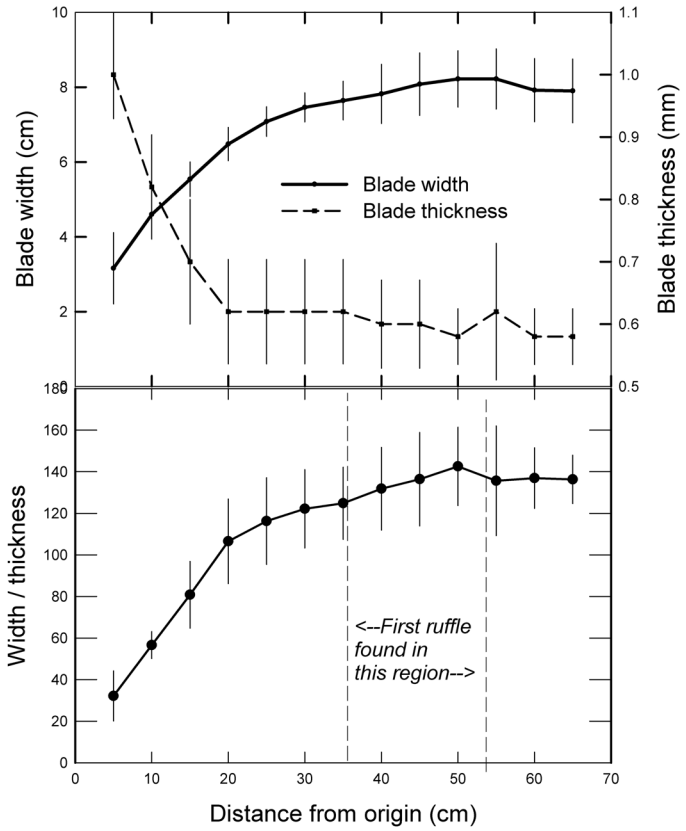

Fig. 5. Blade width and thickness and the dimensionless parameter W/t plotted as a function of distance from the blade origin for ruffled blades from *N. leutkeana* growing at the protected site. Error bars show SDs (n=6 kelp, one blade per kelp). Dashed vertical lines indicate the range of distances from the blade base at which the most recently formed ruffle was observed.

were induced in proximal tissue by the conditions at the sites at which post-transplant growth occurred

Which environmental cues that correlate with flow environment affect growth kinematics and blade ruffling?

Blades on kelp from both flow habitats that were hung with weights mimicking the drag they would experience in a 1.5 m s^{-1} current at a fast-flow site developed uniform growth strains across the width of the blade (Fig. 6B), and there was no significant difference between growth velocities of lateral and midline tissue (paired t-test for growth velocities in the growth zone: P=0.29, n=one blade on each of five kelp from the calm site, df=4; P=0.43, n=one blade on each of five kelp from the fast-flow site, df=4). In contrast, blades on kelp collected from both calm and fast-flow habitats that were grown in tanks without weights or current had higher growth velocities in lateral in than midline tissue (paired t-test for growth velocities in the growth zone: P=0.003, n=one blade on each of 11 kelp from the calm site, df=10; P=0.01, n=one blade on each of 10 kelp from the fast-flow site, df=9). Without weights or rapid current, kelp blades developed transverse growth gradients (Fig. 6), and ruffles (as defined in Fig. 2) formed. Thus drag of ocean currents is identified as a major environmental cue repressing ruffling.

Nutrients were stored in blade tissues from both field sites, indicating that nutrients were not limiting at either site. Nitrate concentrations in blade tissue from kelp growing at the current-swept site (mean=14.9 μM, SD=8.4, n=7 kelp) were not different from concentrations in blade tissue from the protected site (mean=18.8 μM, SD=10.9, n=7 kelp) (Student's t-test, P=0.32, df=12). Similarly, phosphate concentrations in blade tissue from the current-swept (mean=2.8 μM, SD=0.5 n=3 kelp) and protected (mean=2.9 μM, SD=0.7, n=3 kelp) sites were not different (Student's t-test, P=0.85, df=4). Because nutrient storage was similar in kelp from both sites, we conclude that nitrate and phosphate are not environmental cues for ruffling.

Shaded blades grew more slowly than did unshaded blades, but did not develop the growth pattern of strap-like blades at fast-flow sites. Instead, shaded blades with no weights in still water showed higher growth velocities in lateral tissue than along the midline, for kelp collected both from the fast-current site (paired t-test for growth velocities in the growth zone: P=0.04, n=one blade on each of five kelp, df=4) and from the slow-flow site (paired t-test for growth velocities in the growth zone: P=0.02, n=one blade on each of six kelp, df=5) (Fig. 6C). Thus shading is not an environmental cue to suppress ruffling.

Discussion

Following ruffles with time as they grew in a slow-flow habitat, we determined that ruffles form near the base of the blade and then are displaced distally as tissue proximal to them grows. Knowing the timing and location of ruffle formation is the first step in understanding how ruffles are formed and indicates blade regions where physiological mechanisms should be studied. Figures 1, 4 and 5 reveal the interplay of growth kinematics and mechanical constraints in the kelp blade: ruffles are indeed produced by elastic buckling when the edge grows more than the midline. Interestingly, the transverse gradient in growth arises in young, flat tissue (10 cm from the stipe), but only leads to elastic buckling and ruffle formation when the blade has grown wide and thin enough. Thus, ruffles first appear at positions ≥35 cm from the blade base, after another 12 d of growth.

Theoretical analysis of elastic ribbons has identified the patterns of buckling that occur when ribbons of given widths (W) and thicknesses (t) have a transverse growth gradient (ε) that is uniform along their length (Koehl *et al.*, 2008; Liang and Mahadevan, 2009). This elasticity theory predicts that ruffling

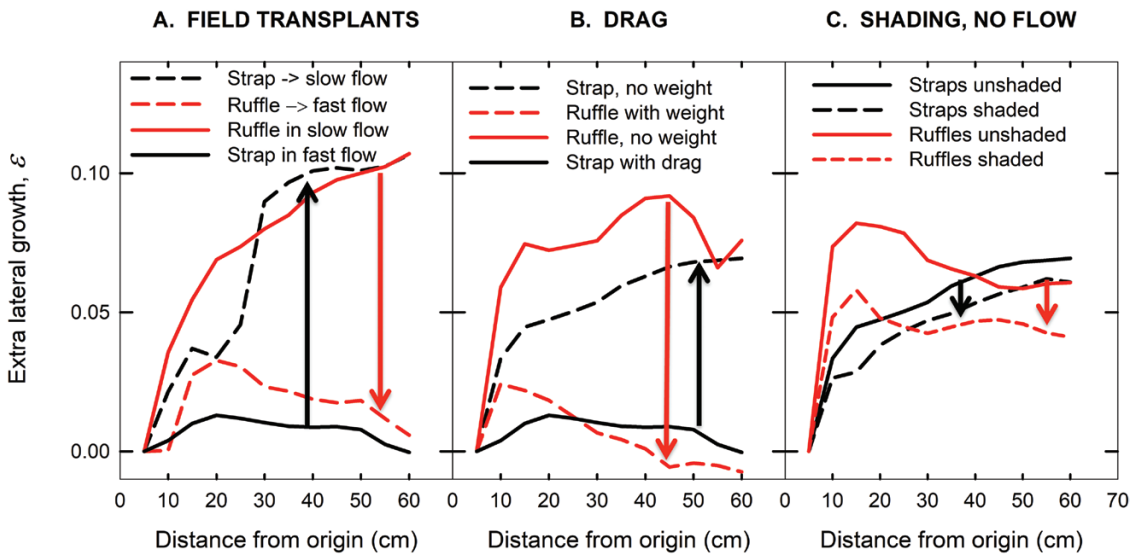

Fig. 6. Effects of environmental variables on extra lateral growth. Arrows indicate the direction of change induced by the experimental treatment. (A) Transplanting strap-like blades from fast (solid black line) to slow (dashed black line) flow induced more growth in lateral tissue than along the midline (ε; Materials and methods) (means of values computed from growth velocities for *n*=one blade on each of four kelp, as described in the Materials and methods), whereas transplanting ruffled blades from slow (solid red line) to fast (dashed red line) current repressed transverse growth gradients (means of values computed from growth velocities for *n*=one blade on each of six kelp, as described in the Materials and Methods). (B) In still water, blades on kelp from both sites showed little transverse growth gradient when weights mimicking drag in a current of 1.5 m s^{-1} were hung on them, but did show extra lateral growth without weights. (C) Low light slowed overall growth rates, but both shaded and unshaded kelp developed transverse growth gradients in still tanks. (Means of values computed from growth velocities for *n*=one blade from each of five kelp from a fast-flow site and from each of six kelp from a calm site. Tests of significance were based on velocity data; see the Results.)

in a ribbon is likely to occur when ε and the ratio of blade width to thickness (W/t) both exceed certain values. Unlike a ribbon with uniform ε (e.g. Liang and Mahadevan, 2009), *N. leutkeana* develops a transverse growth gradient only near the proximal end of the blade. Still, predictions for elastic ribbons with a uniform ε are relevant in determining whether the gradients shown here in the growth zone, considering only two-dimensional growth patterns, are sufficient to produce ruffles. Indeed, the location where we observed formation of the first ruffle has extra lateral growth ε in the range 0.09–0.10 and W/t in the range 138–156, in agreement with theory of elastic ribbons (fig. 4 in Liang and Mahadevan, 2009).

A diversity of mechanisms produce curved forms in thin biological structures. For example, *Antirrhinum* leaves and sweet pea petals ruffle when the tip and central basal tissue stop growing before the basal margins (Nath *et al.*, 2003; Woollacott *et al.*, 2019). The TCP transcription factor CINCINNATA or CYCLOIDEA is involved in the delayed growth arrest of the margins. Undulations in tulip leaves are quite different. The ruffles vary in space and time; they occur as traveling waves produced by spatial oscillation in the pH of the epidermal cell walls (Hejnowicz, 1992). Another mechanism produces the characteristic curvature of the mature maize leaf. The built-in longitudinal curvature is provided mostly by the midrib and has been related to a greater density of fibers on the abaxial side of the leaf (Moulia *et al.*, 1994; Hay *et al.*, 2000). These fibers shorten during their development to cause the downward curve. In mature leaves under water stress, transverse curvature (leaf rolling) occurs when specialized cells on the leaf surface swell (e.g. Gao *et al.*, 2019), which simultaneously causes straightening of the leaves (Moulia, 2000). Thus the longitudinal curvature of the maize and rice leaves is affected by both genes regulating fiber placement and by environmental cues that shrink or swell sensitive epidermal cells. For maize and rice, this is an agronomically important trait that confers resistance to water stress because the rolled, erect leaf is subject to less solar radiation and loses less water. In contrast to the leaf examples cited, ruffling in blades of *Nereocystis* is produced or repressed by an environmental cue that affects growth rates in width and also alters the gradient in longitudinal growth at the blade margins relative to the midline..

We found that the stress due to drag imposed by ocean currents is the major environmental cue affecting transverse growth gradients, thereby repressing or producing ruffles, whereas shading slows the overall growth rate but does not inhibit transverse growth gradients. Ruffling has adaptive significance. The same set of genes produces a beneficial large exposed photosynthetic area in calm water while greatly reducing the harm of drag-induced breakage in swift currents. The resilience of the kelp lies in the ability of the meristematic tissue to respond to the environmental cues. Watching the blade development, we become aware that even though the meristematic tissue responds right away to an environmental cue, the mature blade needs >3 weeks to acquire the adaptive

morphology. During this time, the tissue formed in response to the environmental cue is displaced to distal regions, while the oldest mature tissue erodes away from the distal end of the blade as spore-bearing sori are shed.

The mechanism by which longitudinal mechanical stresses in a kelp blade are transduced into transverse growth gradients is not yet known, but the Lagrangian quantification of growth patterns enables us to identify the location of tissues in blades that should be studied. For example, could drag-induced stress or strain cause greater calcium loss from the walls of tissue near the edges of blades and an interaction with the pectate cycle shown to regulate growth rate in the green alga *Chara* (Proseus and Boyer, 2007)? Rabille *et al.* (2019) have shown that the brown alga *Ectocarpus* regulates the growth rate in tip cells by controlling wall thickness and thereby increasing the turgor-imposed stress in the growing part of the wall. They speculate that wall thickness in turn may be regulated by the delivery of fucans and alginates through vesicle trafficking, and they provide evidence that the highest exocytosis activity is associated with the highest cell wall flux. Thus, it would be interesting to examine whether a transverse gradient in cell wall thickness occurs within the growth zone of the blade of *Nereocystis*, another brown alga. The results of this study show that further work to identify the mechanism of ruffling must focus on the effect of drag on activity in the basal blade tissue and will require demonstration of a transverse gradient in putative growth regulators within the growth zone at the blade base.

Acknowledgements

We thank Friday Harbor Laboratories and the Whitley Center, University of Washington, for use of facilities, C. Baron, N. Pentcheff, H. Stewart, and L. Waldrop for field assistance, and S. Pieria for data entry. This research was funded by a National Science Foundation grant (OCE-60 0241447), a MacArthur Foundation Fellowship, and the Virginia and Robert Gill Chair (to MK). Research of WS has been supported by the National Science Foundation as well as a project in the Agricultural Experiment Station (CA-D-Law-2116-H).

Author contributions

MARK and WKS jointly designed the project, conducted marking experiments *in situ*, produced the figures, and wrote the article. MARK designed and conducted the experiments to assess the importance of drag, light, and transplantation in causing ruffling (shown in Fig. 5). WKS designed and conducted the numerical analysis of the growth trajectories, tissue segment lengths, and growth gradients.

Data availability

Data supporting the findings of this study are available from either author, M.A.R. Koehl or Wendy K. Silk, upon request.

References

Abbott IAH, Hollenberg GJ. 1976. Marine algae of California. Stanford, CA: Stanford University Press.

Aharoni H, Abraham Y, Elbaum R, Sharon E, Kupferman R. 2012. Emergence of spontaneous twist and curvature in non-euclidean rods: application to *Erodium* plant cells. Physical Review Letters **108**, 238106.

Armon S, Efrati E, Kupferman R, Sharon E. 2011. Geometry and mechanics in the opening of chiral seed pods. Science **333**, 1726–1730.

Bastien R, Guayasamin O, Douady S, Moulia B. 2018. Coupled ultradian growth and curvature oscillations during gravitropic movement in disturbed wheat coleoptiles. PLoS One **13**, e0194893.

Bowling AJ, Vaughn KC. 2009. Gelatinous fibers are widespread in coiling tendrils and twining vines. American Journal of Botany **96**, 719–727.

Burnett NP, Koehl MAR. 2019. Mechanical properties of the wave-swept kelp *Egregia menziesii* change with season, growth rate and herbivore wounds. Journal of Experimental Biology **222**, jeb.190595.

Chen Z, Huang GS, Trase I, Han XM, Mei YF. 2016. Mechanical self-assembly of a strain-engineered flexible layer: wrinkling, rolling, and twisting. Physical Review Applied **5**, 017001.

Elbaum R, Zaltzman L, Burgert I, Fratzl P. 2007. The role of wheat awns in the seed dispersal unit. Science **316**, 884–886.

Erickson RO, Sax KB. 1956. Elemental growth-rate of the primary root of *Zea mays*. Proceedings of the American Philosophical Society **100**, 487–498.

Forterre Y, Skotheim JM, Dumais J, Mahadevan L. 2005. How the Venus flytrap snaps. Nature **433**, 421–425.

Gandar PW. 1983. Growth in root apices. 2. Deformation and rate of deformation. Botanical Gazette **144**, 11–19.

Gao L, Yang G, Li Y, *et al.* 2019. Fine mapping and candidate gene analysis of a QTL associated with leaf rolling index on chromosome 4 of maize (*Zea mays* L.). Theoretical and Applied Genetics **132**, 3047–3062.

Gerbode SJ, Puzey JR, McCormick AG, Mahadevan L. 2012. How the cucumber tendril coils and overwinds. Science **337**, 1087–1091.

Green PB. 1976. Growth and cell pattern formation on an axis—critique of concepts, terminology, and modes of study. Botanical Gazette **137**, 187–202.

Hay JO, Moulia B, Lane B, Freeling M, Silk WK. 2000. Biomechanical analysis of the Rolled (RLD) leaf phenotype of maize. American Journal of Botany **87**, 625–633.

Hejnowicz Z. 1992. Traveling pattern of acidity in the epidermis of tulip leaves. Botanica Acta **105**, 266–272.

Hunter T. 1988. Mechanical design of hydroids: flexibility, flow forces and feeding in *Obelia longissima*. Berkeley, CA: University of California.

Hurd CL. 2000. Water motion, marine macroalgal physiology, and production. Journal of Phycology **36**, 453–472.

Isnard S, Cobb AR, Holbrook NM, Zwieniecki M, Dumais J. 2009. Tensioning the helix: a mechanism for force generation in twining plants. Proceedings of the Royal Society B: Biological Sciences **276**, 2643–2650.

Isnard S, Silk WK. 2009. Moving with climbing plants from Charles Darwin's time into the 21st century. American Journal of Botany **96**, 1205–1221.

Jakubska-Busse A, Janowicz M, Ochnio L, Jackowska-Zduniak B. 2016. Shapes of leaves with parallel venation. Modelling of the *Epipactis* sp. (Orchidaceae) leaves with the help of a system of coupled elastic beams. PeerJ **4**, e2165.

Johnson AS, Koehl MAR. 1994. Maintenance of dynamic strain similarity and environmental-stress factor in different flow habitats—thallus allometry and material properties of a giant-kelp. Journal of Experimental Biology **195**, 381–410.

Koehl MAR. 1986. Seaweeds in moving water: form and mechanical function. In: Givnish TJ, ed. On the economy of plant form and function. Cambridge: Cambridge University Press, 603–634.

Koehl MAR, Alberte RS. 1988. Flow, flapping, and photosynthesis of *Nereocystis luetkeana*—a functional comparison of undulate and flat blade morphologies. Marine Biology **99**, 435–444.

Koehl MAR, Quillin KJ, Pell CA. 2000. Mechanical design of fiber-wound hydraulic skeletons: the stiffening and straightening of embryonic notochords. American Zoologist **40**, 28–41.

Koehl MA, Silk WK, Liang H, Mahadevan L. 2008. How kelp produce blade shapes suited to different flow regimes: a new wrinkle. Integrative and Comparative Biology **48**, 834–851.

Liang H, Mahadevan L. 2009. The shape of a long leaf. Proceedings of the National Academy of Sciences, USA **106**, 22049–22054.

Liang H, Mahadevan L. 2011. Growth, geometry, and mechanics of a blooming lily. Proceedings of the National Academy of Sciences, USA **108**, 5516–5521.

Lyndon RF. 1990. Plant development: the cellular basis. London: Unwin Hyman.

Meroz Y, Bastien R, Mahadevan L. 2019. Spatio-temporal integration in plant tropisms. Journal of the Royal Society, Interface **16**, 20190038.

Moulia B. 2000. Leaves as shell structures: double curvature, autostresses, and minimal mechanical energy constraints on leaf rolling in grasses. Journal of Plant Growth Regulation **19**, 19–30.

Moulia B, Fournier M, Guitard D. 1994. Mechanics and form of the maize leaf—in-vivo qualification of flexural behavior. Journal of Materials Science **29**, 2359–2366.

Nath U, Crawford BC, Carpenter R, Coen E. 2003. Genetic control of surface curvature. Science **299**, 1404–1407.

Phyo P, Wang T, Kiemle SN, O'Neill H, Pingali SV, Hong M, Cosgrove DJ. 2017. Gradients in wall mechanics and polysaccharides along growing inflorescence stems. Plant Physiology **175**, 1593–1607.

Proseus TE, Boyer JS. 2007. Tension required for pectate chemistry to control growth in *Chara corallina*. Journal of Experimental Botany **58**, 4283–4292.

Rabille H, Billoud B, Tesson B, Le Panse S, Rolland É, Charrier B. 2019. The brown algal mode of tip growth: keeping stress under control. PLoS Biology **17**, e2005258.

Rivière M, Corre Y, Peaucelle A, Derr J, Douady S. 2020. The hook shape of growing leaves results from an active regulatory process. Journal of Experimental Botany **71**, 6408–6417.

Sharon E, Roman B, Marder M, Shin GS, Swinney HL. 2002. Mechanics. Buckling cascades in free sheets. Nature **419**, 579.

Sharon E, Roman B, Swinney HL. 2007. Geometrically driven wrinkling observed in free plastic sheets and leaves. Physical Review. E, Statistical, Nonlinear, and Soft Matter Physics **75**, 046211.

Silk WK. 1984. Quantitative descriptions of development. Annual Review of Plant Physiology and Plant Molecular Biology **35**, 479–518.

Silk WK, Erickson RO. 1978. Kinematics of hypocotyl curvature. American Journal of Botany **65**, 310–319.

Silk WK, Erickson RO. 1979. Kinematics of plant growth. Journal of Theoretical Biology **76**, 481–501.

Silk WK, Hubbard M. 1991. Axial forces and normal distributed loads in twining stems of morning glory. Journal of Biomechanics **24**, 599–606.

Thompson DAW. 1917. On growth and form. Cambridge: Cambridge University Press.

Wheeler WN, Smith RG, Srivastava LM. 1984. Seasonal photosynthetic performance of *Nereocystis luetkeana*. Canadian Journal of Botany-Revue Canadienne De Botanique **62**, 664–670.

Wolgemuth CW, Inclan YF, Quan J, Mukherjee S, Oster G, Koehl MA. 2005. How to make a spiral bacterium. Physical Biology **2**, 189–199.

Woollacott C, Wang L, Beyer ST, Walus K, Cronk QCB. 2019. CYCLOIDEA gene activity, local growth and curvature in the dorsal petal of *Lathyrus odoratus* (Fabaceae). Botany Letters **166**, 64–69.

Zhao H, Li K, Han M, *et al.* 2019. Buckling and twisting of advanced materials into morphable 3D mesostructures. Proceedings of the National Academy of Sciences, USA **116**, 13239–13248.